Letter

Extraction of the Coulomb sum rule, transverse enhancement, and longitudinal quenching from an analysis of all available e-^{12}C and e-^{16}O cross section data

A. Bodek [1,*] and M. E. Christy [2]

[1] *Department of Physics and Astronomy, University of Rochester, Rochester, New York 14627, USA*

[2] *Thomas Jefferson National Accelerator Facility, Newport News, Virginia 23606, USA*

(Received 1 September 2022; accepted 26 October 2022; published 19 December 2022)

We report on a phenomenological analysis of all available electron scattering data on ^{12}C (about 6600 differential cross section measurements) and on ^{16}O (about 250 measurements) within the framework of the quasielastic (QE) superscaling model (including Pauli blocking). All QE and inelastic cross section measurements are included down to the lowest momentum transfer $\mathbf{q}$ (including photoproduction data). We find that there is enhancement of the transverse QE response function (R_T^{QE}) and quenching of the QE longitudinal response function (R_L^{QE}) at low $\mathbf{q}$ (in addition to Pauli blocking). We extract parametrizations of a *multiplicative* low $\mathbf{q}$ "longitudinal quenching factor" and an *additive* "transverse enhancement" contribution. Additionally, we find that the excitation of nuclear states contribute significantly (up to 30%) to the Coulomb sum rule $SL(\mathbf{q})$. We extract the most accurate determination of $SL(\mathbf{q})$ to date and find it to be in disagreement with random phase approximation (RPA) based calculations but in reasonable agreement with recent theoretical calculations, such as "first principle Green's function Monte Carlo."

DOI: 10.1103/PhysRevC.106.L061305

We report on a fit to all available electron scattering data on ^{12}C (about 6600 differential cross section measurements) and ^{16}O (about 250 measurements) within the framework of the quasielastic (QE) superscaling model (including Pauli blocking). The cross section measurements include the available data on QE [down to the lowest momentum transfer $\mathbf{q}$ ($\equiv |\vec{q}|$)], inelastic production, and photoproduction. The fit includes inelastic structure functions and empirical parameters to model both an enhancement of the transverse (T) QE response function R_T^{QE} and quenching of the longitudinal (L) QE response function R_L^{QE} at low $\mathbf{q}$. As the fit provides an accurate description of all available data, it can be used as a proxy to validate modeling of cross sections in Monte Carlo event generators for electron and neutrino ($\nu_{e,\mu}$) scattering. Careful consideration of nuclear excitations is critical for an accurate extraction of the normalized Coulomb sum rule [1] $SL(\mathbf{q})$ at low $\mathbf{q}$ as these states can contribute up to 29%. After accounting for the dominant excitations, we extract the most accurate determination of $SL(\mathbf{q})$) as function of $\mathbf{q}$ for ^{12}C and ^{16}O based on the global fit and compare to theoretical models. In addition, the "transverse enhancement" (TE) of R_T^{QE} and the "quenching factor" of R_L^{QE} are also of great interest to $\nu_{e,\mu}$ scattering experiments [2–5].

*bodek@pas.rochester.edu

The electron scattering differential cross section can be written [6] in terms of $R_L(\mathbf{q}, \nu)$ and $R_T(\mathbf{q}, \nu)$ as

$$\frac{d^2\sigma}{d\nu\, d\Omega} = \sigma_M[AR_L(\mathbf{q}, \nu) + BR_T(\mathbf{q}, \nu)],$$
$$\sigma_M = \alpha^2 \cos^2(\theta/2)/\left[4E_0^2 \sin^4(\theta/2)\right]. \quad (1)$$

Here, E_0 is the incident electron energy, E' and θ are energy and angle of the final state electron, $\nu = E_0 - E'$, Q^2 is the square of the four-momentum transfer (defined to be positive), $\mathbf{q^2} = \mathbf{Q^2} + \nu^2$, $A = (Q^2/\mathbf{q^2})^2$, and $B = \tan^2(\theta/2) + Q^2/2\mathbf{q}^2$. In the analysis we also use the invariant hadronic mass $W^2 = M_p^2 + 2M_p\nu - Q^2$.

The inelastic Coulomb sum rule is the integral of $R_L(\mathbf{q}, \nu)d\nu$, *excluding the elastic peak and pion production processes*. It has contributions from QE scattering and from electroexcitations of nuclear states:

$$\mathrm{CSR}(\mathbf{q}) = \int R_L(\mathbf{q}, \nu)d\nu$$
$$= \int R_L^{QE}(\mathbf{q}, \nu)d\nu + G_E'^2(Q^2) \times Z^2 \sum_{\mathrm{all}}^{L} F_i^2(\mathbf{q})$$
$$= G_E'^2(Q^2) \times \left[Z \int V_L^{QE}(\mathbf{q}, \nu)d\nu + Z^2 \sum_{\mathrm{all}}^{L} F_i^2(\mathbf{q})\right]. \quad (2)$$

We define $V^{QE}(\mathbf{q}, \nu)$ as the reduced longitudinal QE response, which integrates to unity in the absence of any suppression (e.g., Pauli blocking). The charge form factors for the electroexcitation of nuclear states $F_{iC}^2(\mathbf{q})$ are $G_{Ep}^2(Q^2) \times F_i^2(\mathbf{q})$.

In order to account for the small contribution of the neutron and relativistic effects, $G_E'^2(Q^2)$ is given by [6]

$$G_E'^2(Q^2) = \left[G_{Ep}^2(Q^2) + \frac{N}{Z}G_{En}^2(Q^2)\right]\frac{1+\tau}{1+2\tau}, \quad (3)$$

where G_{Ep} and G_{En} are the electric form factors [7] of the proton and neutron respectively and $\tau = Q^2/4M_p^2$. By dividing Eq. (2) by $ZG_E'^2\mathbf{q}$) we obtain the normalized inelastic Coulomb sum rule $SL(\mathbf{q})$:

$$SL(\mathbf{q}) = \int V_L^{QE}(\mathbf{q}, \nu)d\nu + Z\sum_{\text{all}}^{L} F_i^2(\mathbf{q}). \quad (4)$$

At high $\mathbf{q}$ it is expected that $S_L \to 1$ because both nuclear excitation form factors and Pauli suppression are small. At small $\mathbf{q}$ it is expected that $S_L \to 0$ because all form factors for inelastic processes (QE and nuclear excitations) must be zero at $\mathbf{q} = \mathbf{0}$.

We begin by parametrizing the measurements of the L and T form factors for the electroexcitation of all nuclear states in ^{12}C with excitation energies (E_x) less than 16.0 MeV (the approximate proton removal energy from ^{12}C). For these states the measurements are straightforward since the QE cross section is zero for $E_x < 16$ MeV.

For $E_x > 16$ MeV the extractions of form factors require corrections for the QE contribution. We perform a reanalysis of all published cross sections with in $E_x < 55$ MeV and use our fitted QE model (described below) to extract L and T form factors. For $E_x > 20$ MeV (region of the giant dipole resonances) we group the strength from multiple excitations into a few states with a large width E_x and extract effective form factors accounting for all states in this region. The top two panels of Fig. 1 show comparisons of our fit (red) to R_L measurements by Yamaguchi (blue) 1996 [8] with $E_x > 14$ MeV. An estimated resolution smearing of 600 keV has been applied to the excitations in the fit to match the data. While individual states are well reproduced at low excitation energy, above 20 MeV the effect of grouping several excitations together into broad effective states in the fit can be seen. While the fit does not capture the structure from individual states, the total strength is well reproduced. A similar analysis has been done for ^{16}O.

The contribution of nuclear excitation to $SL(\mathbf{q})$ [factor $Z\sum_{\text{all}}^{L} F_i^2(\mathbf{q})$ in Eq. (4)] is calculated using the parametrizations of the form factors. The bottom panel of Fig. 1 shows the contributions of nuclear excitations to $SL(\mathbf{q})$ for ^{12}C. The contribution of all excitations is largest (≈ 0.29) at $\mathbf{q} = \mathbf{0.22}$ GeV. Although the contributions of different E_x regions to $SL(\mathbf{q})$ is different for ^{12}C and ^{16}O, the total contribution turns out to be similar for the two nuclei. The total contribution of excitations to $S_L(\mathbf{q})$ in ^{12}C can be parametrized as:

$$Z\sum_{\text{all}}^{L} F_i^2(\mathbf{q}) = N_1 e^{-(x-C_1)^2/D_1^2} + N_2 e^{-(x-C_2)^2/D_2^2} + N_3 e^{-(x-C_3)^2/D_3^2}, \quad (5)$$

where $x = \mathbf{q}/K_F$ ($K_F = 0.228$ GeV); $N_1 = 0.260$, $C_1 = 1.11$, $D_1 = 0.50$; $N_2 = 0.075$, $C_2 = 0.730$, $D_2 = 0.30$; and $N_3 =$

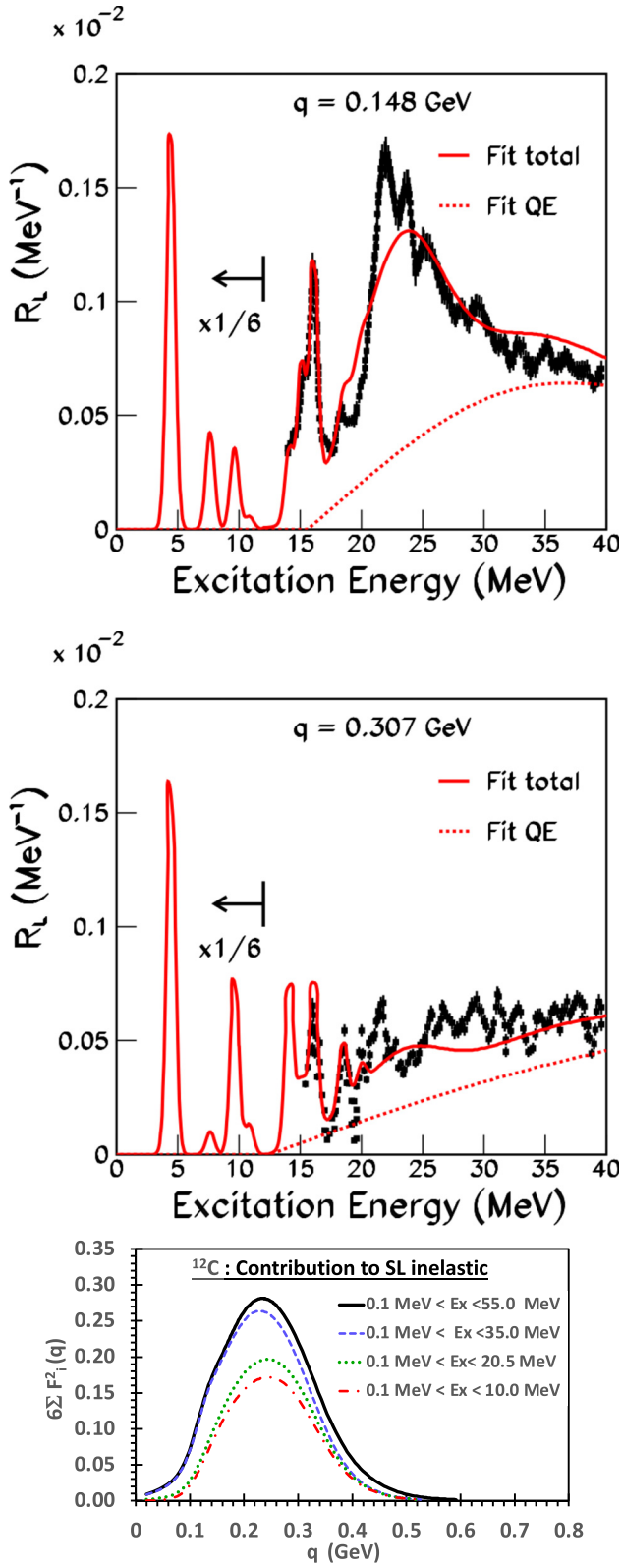

FIG. 1. Top two panels: Comparison of $R_L(\mathbf{q}, \nu)$ extracted from our ^{12}C fit (solid red) to a sample of experimental data (black points) [8]. The QE contribution is shown as the dashed red line. For E_x less than 12 MeV the values are multiplied by 1/6. Bottom panel: The contributions of longitudinal nuclear excitations (between 2 and 55 MeV) to the Coulomb sum rule [$Z\sum_{\text{all}}^{L} F_i^2(\mathbf{q})$] in Eq. (4) for ^{12}C.

0.01, $C_3 = 2.0$, $D_3 = 0.30$. The uncertainty in the total contribution of excited states was estimated to be 15% plus a systematic error to account for the choice of parametrization at very low $\mathbf{q}$ (± 0.01) added in quadrature. The universal fit to the ^{12}C data is an update of the 2012 fit by Bosted and Mamyan [9]. The QE contribution is modeled by the superscaling approach [10–13] with Pauli blocking calculated using the Rosenfelder [13–15] method. The superscaling function extracted from the fit is similar to the superscaling functions of Amaro 2005 [11] and Amaro 2020 [12] and yields similar Pauli suppression.

In modeling the QE response we use the same scaling function for both $R_L^{QE}(\mathbf{q}, \nu)$ and $R_T^{QE}(\mathbf{q}, \nu)$ and fit for empirical corrections to the response functions. For R_T^{QE} we extract an *additive* "transverse enhancement/Meson Exchange Currents (MEC)'' TE($\mathbf{q}, \nu$) contribution (which includes both single nucleon and two nucleon final states). As shown in Ref. [16]. TE($\mathbf{q}, \nu$) increases R_T^{QE} with the largest fractional contribution around $Q^2 = 0.3$ GeV^2. For R_L^{QE} we extract a *multiplicative* $\mathbf{q}$ dependent "longitudinal quenching factor," $F_{\rm quench}(\mathbf{q})$, which decreases R_L^{QE} at low $\mathbf{q}$.

Since $\frac{d^2\sigma}{d\Omega\, d\nu}$ measurements span a large range of θ and $\mathbf{q}$, parametrizations of both TE($\mathbf{q}, \nu$) and $F^L_{\rm quench}(\mathbf{q})$ can be extracted. The analysis includes all data for a large range of nuclei. However, in this paper we only include data on ^{12}C and ^{16}O. Briefly, the updated fit includes

(1) All electron scattering data on ^{1}H, ^{2}H, ^{12}C, and ^{16}O in addition to the data in the QE [17] and resonance [18] data archives.
(2) Coulomb corrections [19] using the effective momentum approximation (EMA) in modeling scattering from nuclear targets.
(3) Updated nuclear elastic+excitations form factors.
(4) Superscaling $F N(\psi')$ parameters are reextracted including the Fermi broadening parameter K_F.
(5) Parametrizations of the free nucleon form factors [20] are rederived from all ^{1}H and ^{2}H data.
(6) Rosenfelder Pauli suppression [13–15], which reduces and changes the QE distribution at low $\mathbf{q}$ and ν.
(7) Updates of fits [20] to inelastic electron scattering data (in the nucleon resonance region and inelastic continuum) for ^{1}H and ^{2}H.
(8) A $\mathbf{q}$ dependent $E^{QE}_{\rm shift}(\mathbf{q})$ parameter for the QE process to account for the optical potential [21] of final state nucleons.
(9) Photoproduction data in the nucleon resonance region and inelastic continuum [22].
(10) Gaussian Fermi smeared nucleon resonance and inelastic continuum [22]. The K_F parameters for pion production and QE can be different.
(11) Parametrizations of the medium modifications of both the L and T structure functions responsible for the European Muon Collaboration (EMC) effect (nuclear dependence of inelastic structure functions). These are applied to the free nucleon cross sections prior to application of the Fermi smearing.
(12) Parametizations of TE($\mathbf{q}, \nu$) and $F^L_{\rm quench}(\mathbf{q})$ as described below.
(13) QE data at *all values* of Q^2 down to $Q^2 = 0.01$ GeV^2 ($\mathbf{q} = \mathbf{0.1}$ GeV) (which were not included in the Bosted-Mamyan fit).

The average (over ν) Pauli suppression factor for $x < 2.5$ ($x = \mathbf{q}/K_F$, $K_F = 0.228$ GeV) is described by

$$\left\langle F_{\rm Pauli}^{\rm This\text{-}analysis}(\mathbf{q})\right\rangle = \sum_{j=0}^{j=3} k_j (x)^j. \tag{6}$$

Using the Rosenfeld method with superscaling function used in this analysis, we find $k_o = 0.3054$, $k_1 = 0.7647$, $k_2 = -0.2768$, and $k_3 = 0.0328$. The Pauli suppression factor for $x > 2.5$ is 1.0.

Comparisons of the fit to electron scattering $\frac{d^2\sigma}{d\Omega\, d\nu}$ measurements [17,23,24] at different values of θ for $\mathbf{q}$ values close to 0.30, 0.38, and 0.57 GeV (corresponding to extractions of R_L and R_T by Jourdan [25]) are shown in Fig. 2. Shown are the total $\frac{d^2\sigma}{d\Omega\, d\nu}$ cross section (solid magenta line), the total minus the contribution of nuclear excitations (dot-dashed green), the QE cross section without TE (dashed blue), the TE contribution (thin solid red), and inelastic pion production (dot-dashed black). An estimated resolution smearing of 3.5 MeV has been applied to the excitations to better match the data.

The fit is in good agreement with all electron scattering data for both small and large θ.

The extracted QE "longitudinal quenching factor" $F^L_{\rm quench}(\mathbf{q})$ is unity for $x > 3.75$, and is zero for $x < 0.35$. For $0.35 < x < 4.0$ it is parametrized by

$$F^L_{\rm quench}(\mathbf{q}) = \frac{(x-0.2)^2}{(x-0.18)^2}[1.0 + A_1(3.75-x)^{1.5} + A_2(3.75-x)^{2.5} + A_3(3.75-x)^{3.5}] \tag{7}$$

with $A_1 = -0.13152$, $A_2 = 0.11693$, and $A_3 = -0.03675$. The top-left panel of Fig. 3 shows the extracted $F^L_{\rm quench}(\mathbf{q})$. (black dotted line). The yellow band includes the statistical, parametrization and a normalization error of 2% (all added in quadrature).

If another formalism is used to model QE scattering (e.g., Relativistic Fermi Gas (RFG) or spectral functions) then the quenching factor for the model $F^{L\text{-model}}_{\rm quench}(\mathbf{q})$ is given by

$$F^{L\text{-model}}_{\rm quench}(\mathbf{q}) = \frac{\left\langle F_{\rm Pauli}^{\rm This\text{-}analysis}(\mathbf{q})\right\rangle}{\left\langle F_{\rm Pauli}^{\rm model}(\mathbf{q})\right\rangle} F^L_{\rm quench}(\mathbf{q}) \tag{8}$$

The top right panel of Fig. 3 shows the various contributions to the measured $SL(\mathbf{q})$ for ^{12}C (dotted blue line with yellow error band). Shown are the QE contribution with only Pauli suppression (dotted purple), QE suppressed by both "Pauli suppression" and $F^L_{\rm quench}(\mathbf{q})$ labeled as QE total suppression (solid green), and the contribution of nuclear excitations (red dashed line). The green error band is 15% plus 0.01 added in quadrature.

The left panel on the bottom of Fig. 3 shows a comparison of the extracted $SL(\mathbf{q})$ for ^{12}C (dotted blue curve with yellow error band) to theoretical calculations. These include the Lovato 2016 [27] 'first principle Green's function

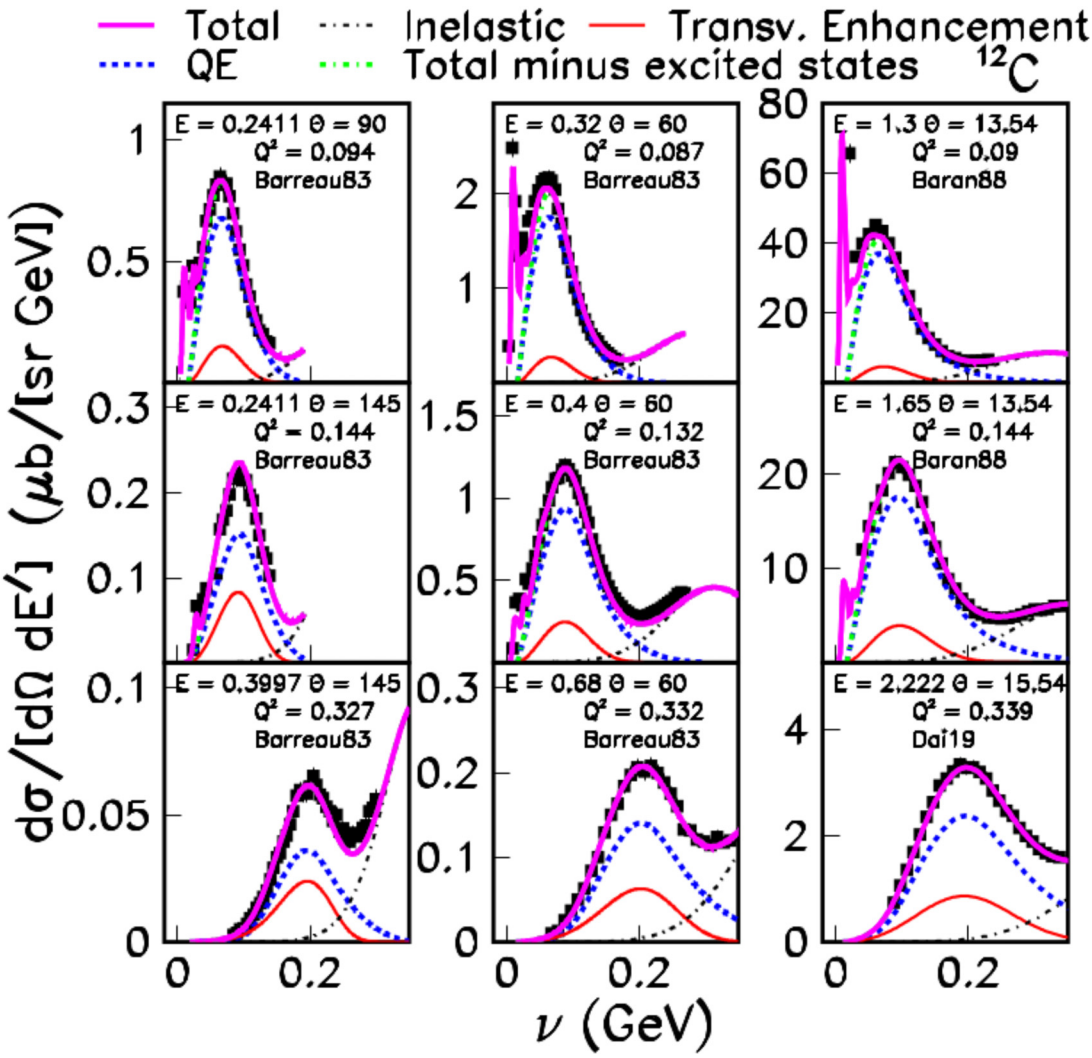

FIG. 2. Comparison of the fit to electron scattering $\frac{d^2\sigma}{d\Omega\, d\nu}$ measurements [17,23,24] at $\mathbf{q}$ values close to 0.30, 0.38, and 0.57 GeV (and different scattering angles). Shown are total $\frac{d^2\sigma}{d\Omega\, d\nu}$ (solid purple line), total minus the contribution of the nuclear excitations (solid blue), the QE cross section without TE (dashed blue), the TE contribution (solid red), and inelastic pion production (dot-dashed black line). Additional comparisons are included in Supplemental Material [26].

Monte Carlo" (GFMC) calculation (solid purple line), Mihaila 2000 [28] coupled-clusters based calculation (AV18+UIX potential, dashed green), and Cloet 2016 [29] RPA calculation (RPA solid red). Our measurements for ^{12}C are in disagreement with Cloet 2016 RPA, and in reasonable agreement with Lovato 2016 and Mihaila 2000 except near $\mathbf{q} \approx 0.30$ GeV where the contribution from nuclear excitations is significant.

There are not enough QE data for ^{16}O to perform a complete analysis. We find that the QE fit parameters for ^{12}C also describe all available data on ^{16}O. A difference in $SL(\mathbf{q})$ between ^{12}C and ^{16}O could be the contribution of nuclear excitations. However we find that the contributions of nuclear excitations to the $SL(\mathbf{q})$ for ^{12}C and ^{16}O are consistent with being equal.

The bottom right panel of Fig. 3 shows $SL(\mathbf{q})$ for ^{16}O (dotted blue with green error band) compared to theoretical calculations. These include the Sobczyk 2020 [30] "coupled cluster with singles and doubles (CCSD) NNLO$_{\rm sat}$" (red dashed line), and Mihaila 2000 [28] coupled-cluster calculation with AV18+UIX potential (dashed green line). The data are in reasonable agreement with Sobczyk 2020 and Mihaila 2000 calculations for ^{16}O except near $\mathbf{q} \approx 0.30$ GeV where the contribution from nuclear excitations is significant.

The TE($\mathbf{q}$, ν) contribution to the QE transverse structure function $F_1(\mathbf{q}, \nu)$ for ^{12}C is parameterized as a distorted Gaussian centered around $W \approx 0.88$ GeV and a second Gaussian at $W \approx 1.2$ GeV [31] with Q^2 dependent width and amplitude. $F_1^{\rm MEC} = 0$ for $\nu < \nu_{\rm min}$ ($\nu_{\rm min} = 16.5$ MeV). For $\nu > \nu_{\rm min}$ it is given by

$$F_1^{\rm MEC} = \max\left[\left(f_1^A + f_1^B\right), 0.0\right],$$
$$f_1^A = a_1 Y\left[\left(W^2 - W_{\rm min}^2\right)^{1.5} e^{-(W^2-b_1)^2/2c_1^2}\right],$$
$$f_1^B = a_2 Y\left(Q^2 + q_o^2\right)^{1.5}\left[e^{-(W^2-b_2)^2/2c_2^2}\right],$$

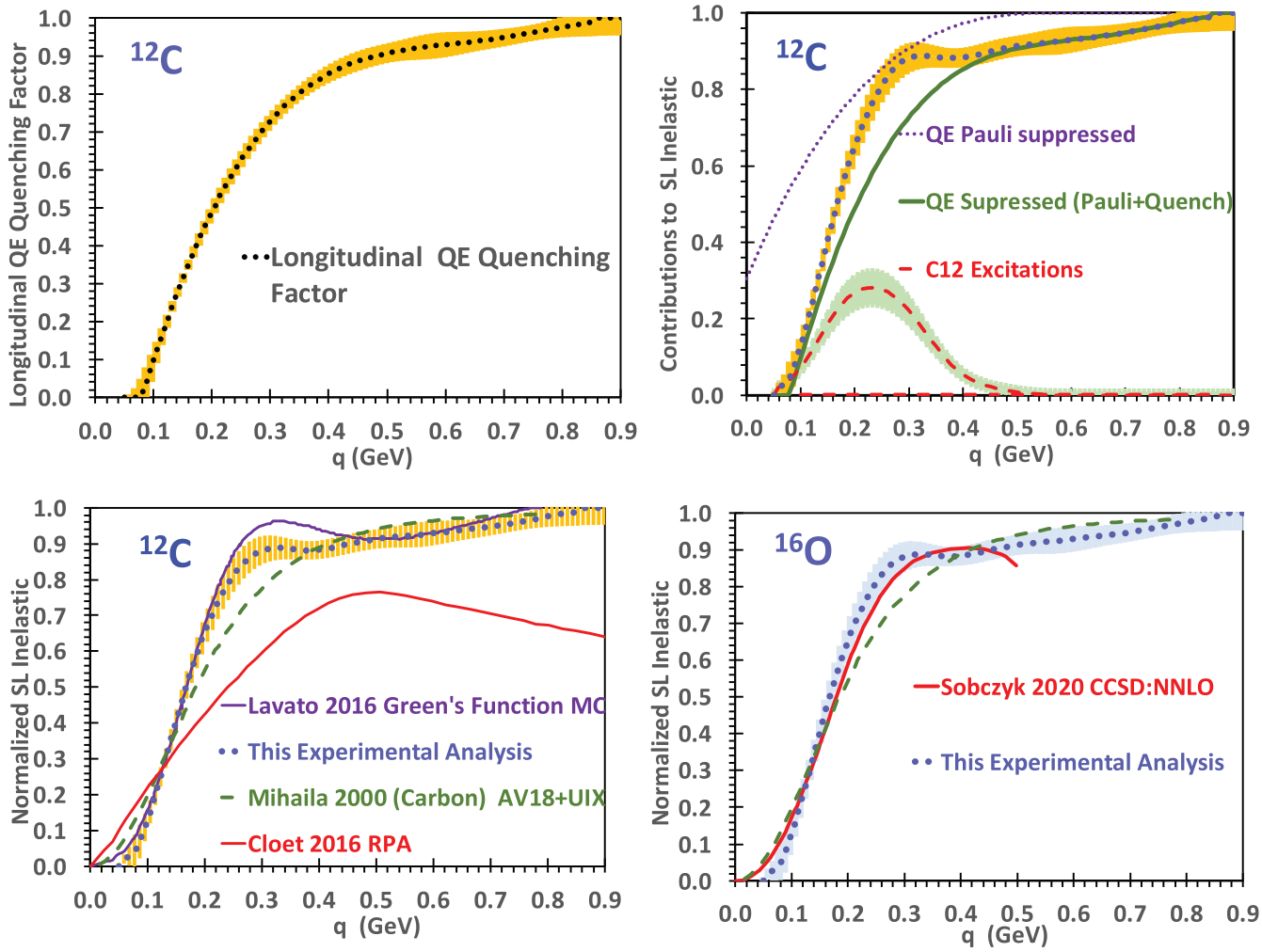

FIG. 3. Top left panel: QE "longitudinal quenching factor" (dotted black line with yellow error band). Top right panel: The various contributions to $SL(\mathbf{q})$ for ^{12}C (dotted blue with yellow error band) including QE with Pauli suppression only (dotted purple), QE suppressed by both "Pauli" and "longitudinal quenching" (solid green), and the contribution of nuclear excitations (red dashed with green error band). Bottom left panel: $SL(\mathbf{q})$ for ^{12}C (dotted blue with yellow error band) compared to theoretical calculations including Lovato 2016 [27] (solid purple), Mihaila 2000 [28] (dashed green), and RPA Cloet 2016 [29] (solid red). Bottom right panel: $SL(\mathbf{q})$ for ^{16}O (dotted black with green error band) compared to theoretical calculations of Sobczyk 2020 [30] (red dashed) and Mihaila 2000 (dot-dashed).

$$Y = Ae^{-Q^4/12.715}\frac{\left(Q^2+q_0^2\right)^2}{(0.13380+Q^2)^{6.90679}},$$
$$a_1 = 0.091\,648, \quad a_2 = 0.10223,$$
$$W_{\min}^2 = M_p^2 + 2M_p\nu_{\min} - Q^2, \tag{9}$$

where Q^2 is in units of GeV^2, M_p is the proton mass, A is the atomic weight, $q_0^2 = 1.0\times10^{-4}$, $b_1 = 0.77023$, $c_1 = 0.077051 + 0.26795Q^2$, $b_2 = 1.275$, and $c_2 = 0.375$.

The parameters of the empirical model of TE($\mathbf{q}$, ν) in electron scattering can be used to predict the TE($\mathbf{q}$, ν) contribution in neutrino scattering [32].

A comparison between our extraction (thick solid blue) of $R_L(\mathbf{q},\nu)$ and $R_T(\mathbf{q},\nu)$ and the extraction (for only three values of $\mathbf{q}$) by Jourdan [25] (data points) are shown in Fig. 4. At the lowest $\mathbf{q}$ our $R_L(\mathbf{q},\nu)$ is somewhat lower and our $R_T(\mathbf{q},\nu)$ is somewhat higher (the Jourdan analysis includes data from only two experiments). Also shown are two one-body + two-body (1b+2b) current calculations: GFMC [27] and "energy-dependent relativistic mean field" (ED-RMF) [33]. In our fit, we show each nuclear excitation with excitation energy E_x at $\nu = E_x + \mathbf{q}^2/2M_{C12}$, where M_{C12} is the mass of the carbon nucleus. In contrast, the ED-RMF calculations group all excitations in two fixed ν peaks as shown in Fig. 4, and the GFMC calculations do not show any nuclear excitations. Both calculations are in reasonable agreement with our analysis in the QE region. In both models there is enhancement of $R_T^{QE}(\mathbf{q},\nu)$ if only 1b currents are included and additional enhancement if both 1b and 2b currents are included. The curves labeled 2b in Fig. 4 show the enhancement in $R_T^{QE}(\mathbf{q},\nu)$ from 2b currents only [i.e., (1b+2b) minus (1b only)], while our empirical extraction of TE($\mathbf{q}$, ν) shown in Fig. 4 models the enhancement in $R_T(\mathbf{q},\nu)$ from all sources.

In summary, using all available electron scattering data we extract parametrizations of the quenching of the $R_L^{QE}(\mathbf{q},\nu)$

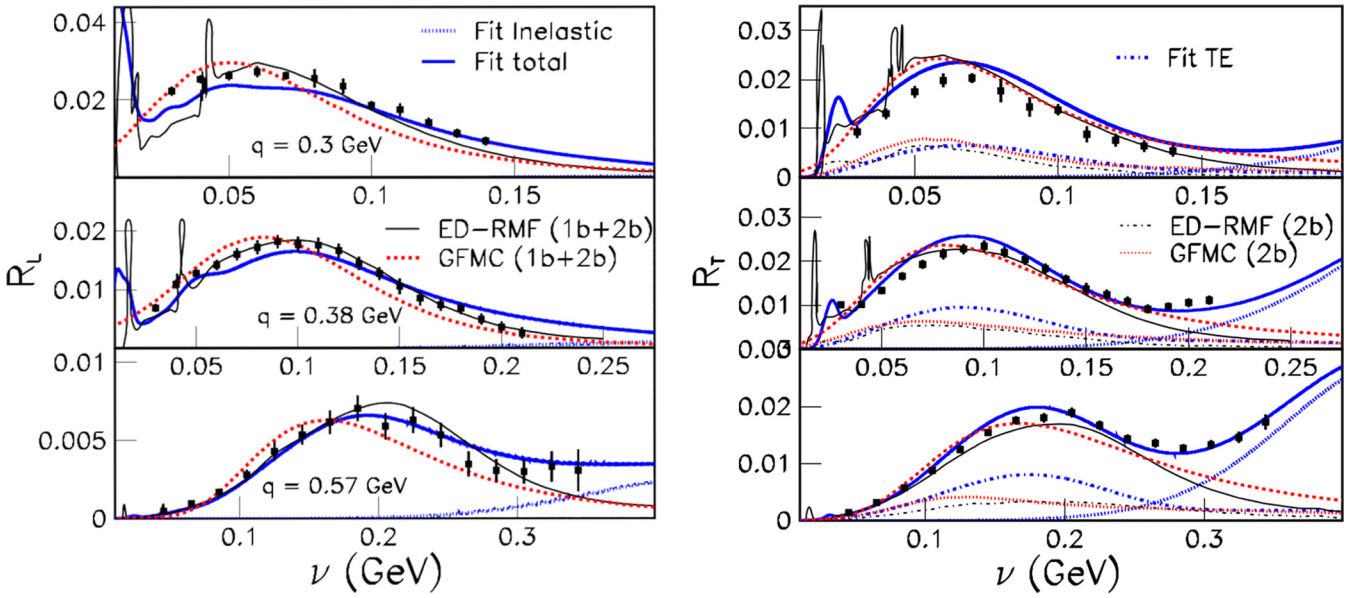

FIG. 4. Comparisons between our extraction of $R_L(\mathbf{q}, \nu)$ and $R_T(\mathbf{q}, \nu)$ and the extraction (for only three values of $\mathbf{q}$) by Jourdan [25] (the Jourdan analysis includes data from only two experiments). Also shown are comparisons to 1b+2b GFMC [27] and ED-RMF [33] theoretical predictions. In these two models the curves labeled 2b are the only contribution of two-body currents to TE($\mathbf{q}$, ν). The transverse enhancement in both 1b and 2b currents is included in the total.

and the enhancement of $R_T^{QE}(\mathbf{q}, \nu)$ over a large range of $\mathbf{q}$ and ν. We obtain the best measurement of the Coulomb sum rule $SL(\mathbf{q})$ to date and compare to theoretical models. The contribution of nuclear excitations to $SL(\mathbf{q})$ is significant (up to 29%). Theoretical studies show that nuclear excitations are also significant in $\nu_{e,\mu}$ scattering [34,35]. Therefore, nuclear excitations should be included in both e-N and ν-N MC generators.

This Research is supported by the U.S. Department of Energy, Office of Science, under University of Rochester Grant No. DE-SC0008475, and the Office of Science, Office of Nuclear Physics under Contract No. DE-AC05-06OR23177.

[1] D. Drechsel and M. M. Giannini, Rep. Prog. Phys. **52**, 1083 (1989), Eq. 7.9; T. de Forest, Jr. and J. D. Walecka, Adv. Phys. **15**, 1 (1966).
[2] A. A. Aguilar-Arevalo *et al.* (MiniBooNE Collaboration), Phys. Rev. Lett. **100**, 032301 (2008).
[3] M. F. Carneiro *et al.* (MINERvA Collaboration), Phys. Rev. Lett. **124**, 121801 (2020).
[4] P. Abratenko *et al.* (MicroBooNE Collaboration), Phys. Rev. Lett. **123**, 131801 (2019).
[5] P. Abratenko *et al.* (MicroBooNE Collaboration), Phys. Rev. Lett. **125**, 201803 (2020).
[6] J. A. Caballero, M. C. Martinez, J. L. Herraiz, and J. M. Udias, Phys. Lett. B **688**, 250 (2010).
[7] A. Bodek, S. Avvakumov, R. Bradford, and H. Budd, Eur. Phys. J. C **53**, 349 (2008).
[8] D. G. Boulware, L. S. Brown, and R. D. Peccei, Phys. Rev. D **3**, 1750 (1971).
[9] P. E. Bosted and V. Mamyan, arXiv:1203.2262; V. Mamyan, Ph.D. dissertation, University of Virginia, 2010 (unpublished).
[10] C. Maieron, T. W. Donnelly, and I. Sick, Phys. Rev. C **65**, 025502 (2002).
[11] J. E. Amaro, M. B. Barbaro, J. A. Caballero, T. W. Donnelly, A. Molinari, and I. Sick, Phys. Rev. C **71**, 015501 (2005).
[12] J. E. Amaro, M. B. Barbaro, J. A. Caballero, R. Gonzalez-Jimenez, G. D. Megias, and I. Ruiz Simo, J. Phys. G: Nucl. Part. Phys. **47**, 124001 (2020).
[13] G. D. Megias Vazquez, Tesis Doctoral, Universidad de Sevilla, 2017 (unpublished).
[14] R. Rosenfelder, Ann. Phys. **128**, 188 (1980).
[15] G. D. Megias, M. V. Ivanov, R. Gonzalez-Jimenez, M. B. Barbaro, J. A. Caballero, T. W. Donnelly, and J. M. Udias, Phys. Rev. D **89**, 093002 (2014).
[16] A. Bodek, H. Budd, and M. Christy, Eur. Phys. J. C **71**, 1726 (2011).
[17] O. Benhar, D. Day, and I. Sick, Rev. Mod. Phys. **80**, 189 (2008).
[18] Resonance Data Archive, https://hallcweb.jlab.org/resdata/
[19] P. Gueye, M. Bernheim, J. F. Danel, J. E. Ducret, L. Lakehal-Ayat, J. M. LeGoff, A. Magnon *et al.*, Phys. Rev. C **60**, 044308 (1999).
[20] P. E. Bosted, Phys. Rev. C **51**, 409 (1995).
[21] A. Bodek and T. Cai, Eur. Phys. J. C **79** 293 (2019); **80**, 655 (2020).
[22] P. E. Bosted and M. E. Christy, Phys. Rev. C **77**, 065206 (2008); M. E. Christy and P. E. Bosted, *ibid.* **81**, 055213 (2010).
[23] P. Barreau *et al.*, Nucl. Phys. A **402**, 515 (1983).

[24] D. T. Baran *et al.*, Phys. Rev. Lett. **61**, 400 (1988).
[25] J. Jourdan, Nucl. Phys. A **603**, 117 (1996); Phys. Lett. B **353**, 189 (1995).
[26] See Supplemental Material at http://link.aps.org/supplemental/10.1103/PhysRevC.106.L061305 for additional comparisons of the universal fit to some of the measurements of $\frac{d^2\sigma}{d\Omega\, d\nu}$ on ^{12}C and ^{16}O.
[27] A. Lovato, S. Gandolfi, J. Carlson, S. C. Pieper, and R. Schiavilla, Phys. Rev. Lett. **117**, 082501 (2016).
[28] B. Mihaila and J. H. Heisenberg, Phys. Rev. Lett. **84**, 1403 (2000).
[29] I. C. Cloët, W. Bentz, and A. W. Thomas, Phys. Rev. Lett. **116**, 032701 (2016).
[30] J. E. Sobczyk, B. Acharya, S. Bacca, and G. Hagen, Phys. Rev. C **102**, 064312 (2020).
[31] A. V. Butkevich and S. V. Luchuk, Phys. Rev. C **102**, 024602 (2020).
[32] K. Gallmeister, U. Mosel, and J. Weil, Phys. Rev. C **94**, 035502 (2016); S. Dolan, U. Mosel, K. Gallmeister, L. Pickering, and S. Bolognesi, *ibid.* **98**, 045502 (2018).
[33] T. Franco-Munoz, R. Gonzalez-Jimenez, and J. M. Udias, arXiv:2203.09996.
[34] V. Pandey, N. Jachowicz, T. Van Cuyck, J. Ryckebusch, and M. Martini, Phys. Rev. C **92**, 024606 (2015),
[35] M. Martini, N. Jachowicz, M. Ericson, V. Pandey, T. Van Cuyck, and N. Van Dessel, Phys. Rev. C **94**, 015501 (2016); V. Pandey, N. Jachowicz, M. Martini, R. Gonzalez-Jimenez, J. Ryckebusch, T. Van Cuyck, and N. VanDessel, *ibid.* **94**, 054609 (2016).